International Journal of Concrete Structures and Materials

RESEARCH

Open Access

Mechanical Properties of Lightweight Aggregate Concrete Reinforced with Various Steel Fibers

Keun-Hyeok Yang, Hak-Young Kim* and Hye-Jin Lee

Abstract

The objective of the present study is to examine the effects of different types and content of steel fibers on the workability, mechanical properties, and ductility enhancement of lightweight aggregate concrete (LWAC). Thirteen LWAC mixtures were prepared using different types of steel fibers including conventional hooked-end macro steel fibers (SF(H)), straight (CSF(S)), crimp-shaped (CSF(C)), and hooked-end (CSF(H)) copper-coated micro steel fibers at the designed compressive strength of 40 MPa. The fiber volume fraction varied from 0% to 1.5% at an interval of 0.5%. Test results showed that CSF(H) type possesses a better potential than the other types in enhancing the tensile resistance and toughness at the post-peak branch of the load–deflection curve of beams. The bond characteristics of fibers with cement matrix were one of critical parameters that needs to be considered in designing the fiber reinforced concrete. Thus, the splitting strength, modulus of rupture, and modulus of elasticity of fiber reinforced LWAC were formulated as a function of volume fraction, aspect ratio, and bond strength of fibers from the regression analysis using the present test data.

Keywords: fiber-reinforced lightweight aggregate concrete, steel fiber, bond stress, mechanical properties, regression analysis

1 Introduction

With the development of large and tall concrete structures, concrete is required to have better performance (e.g., workability, higher strength and toughness, and light weight) (Mays & Barnes, 1991). Lightweight aggregate concrete (LWAC) is superior to normal weight concrete (NWC) in terms of fire resistance, seismic resistance, and thermal insulation (Li et al., 2017). LWAC has a higher strength-to-weight ratio than NWC (ACI Balendran et al., 2002; Committee&213, 2014). Hence, relatively smaller cross-sectional area and lighter structural elements can be designed using LWAC. It is necessary to set the target strength high to offset the low stiffness of LWAC designed for structural purposes. However, an increase in concrete strength can result in high brittleness (Li et al., 2021). The addition of fibers to concrete can mitigate these negative effects and improve the mechanical performance of LWAC (Hamoush et al., 2010). The most important properties of fibers that affect the strength and ductility of LWAC are the volume fraction (V_f), aspect ratio (S_f), tensile strength (F_f), and bond stress (τ) between the cement matrix and fiber interface. Steel fibers are commonly used to improve the mechanical properties of LWAC (Turk et al., 2021). However, if V_f of steel fibers is 2% or more, LWAC density may increase. Furthermore, corrosion of steel fibers may decrease the long-term durability of concrete. Alternatively, copper-coated micro steel fibers having a diameter (d_f) of approximately 0.2 mm can be used (Okeh et al., 2019). In general, fibers with smaller d_f and larger S_f can secure

Journal information: ISSN 1976-0485 / eISSN2234-1315

*Correspondence: concrete@kyonggi.ac.kr

Department of Architectural Engineering, Kyonggi University, Suwon, Gyonggi-do, South Korea

the ductility of concrete even with a relatively low V_f. Moreover, surface coating can help in long-term corrosion resistance.

Kang et. al. (2010) reported that the tensile strength of ultra high performance fiber reinforced concrete increases linearly when the V_f of the steel fibers is increased up to 5%. Dupont and Vandewalle (2005) pointed out that when V_f exceeded 2%, the interaction between fibers increased. This could induce a balling effect during the mixing or placing process of concrete. Park et. al. (2012) and Kim et. al. (2011) showed that deformed macro steel fibers (twisted, crimped, and hooked-end shapes) could significantly improve the tensile and flexural performance of concrete compared to non-deformed steel fibers (e.g., straight shape). The deformed shape can increase the fiber pullout resistance in the cement matrix, and it could be directly related to the improvement of the bridging effect of the fibers (Wu et al., 2018). Visalvanich and Naaman (1983) indicated that there was a concern that the deformed shapes of steel fibers could act as a link to weave other fibers during the mixing process. This could inhibit the distribution of fibers. As a result, the geometry of the steel fiber can lead to contradictory results in assessing the workability, tensile capacity and mechanical properties of concrete. Hence, shape of fiber should be considered as a critical parameter along with V_f in assessing the mechanical properties of concrete. Additional studies on fiber reinforced lightweight aggregate concrete (FRLWAC) are needed because of the variability in the characteristics of lightweight aggregates (LWAs). In LWAC, cracks and fractures first occur in the aggregates unlike NWC, where the performance of the concrete is mainly determined by the paste, because the aggregate is generally stronger than the paste (Sim et al., 2013). Lee et. al. (2019) reported that the low strength of the lightweight aggregates yields more rapid crack propagation and more brittle fracture of concrete, because the cracks mainly pass through the aggregate particles, resulting in localized failure zones. Therefore, a large amount of data on the mechanical properties of FRLWAC is needed to establish a design model for making detailed decisions (e.g., fiber type, V_f and LWA type, density, and water absorption) to achieve the target performance of FRLWAC.

In this study, we evaluated the effects of various properties of different fibers on the mechanical properties of FRLWAC. Four steel fiber types with different geometrical shapes, L_f, and d_f were used in this study. Twelve FRLWAC mixtures were prepared for different V_f. A fiberless mixture was used as a control group. The compressive strength ($f_c(t)$), splitting tensile strength (f_{sp}), load–deflection relationship, modulus of rupture (f_r) of concrete, and bond stress–slip relationship of embedded individual fibers were evaluated in this study. In addition, equations were developed based on experimental data and regression analysis to comprehensively evaluate the various mechanical properties of FRLWAC.

2 Experimental Details

2.1 Materials and Mix Proportion

The ordinary Portland cement used in this study had a density of 3.15 g/cm^3 and a specific surface area of 3260 cm^2/g with other properties meeting the specifications of ASTM type I (2012) (ASTM C150/C150M, 2011). Commercially available artificially expanded granules manufactured by Korea South–East Power Co. were used as structural LWAs. The bottom ash and dredged soil used for the raw materials of the granules were calcined and allowed to expand in large rotary kilns at approximately 1200 °C. The main components of the LWA, confirmed by X-ray diffraction, were quartz and magnetite (Fig. 1). The expanded granules were produced in nominal sizes (e.g., below 2 mm, 2–5 mm, 5–10 mm, and 10–20 mm), and adjusted to satisfy the particle distribution curve specified in ASTM C 330 (ASTM C330/C330M, 2017). The physical characteristics of the LWAs used are summarized in Table 1. In this study, four types of steel fibers with different shapes, surface coating conditions, L_f, d_f, and τ were used. In addition, different copper-coated fibers (i.e., straight (CSF(S)), crimped (CSF(C)), and end-hooked (CSF(H)) in addition to conventional end-hooked steel fibers (SF(H)) were utilized (Fig. 2). The manufacturer (SM KOREA Co., Anyang-si, Korea) reported that the tensile strengths of SF and CSF were 2240 and 1220 MPa, respectively. Additional fiber properties are shown in Table 2.

Table 3 shows the mix proportion of LWAC used in the experiment. The water-to-cement ratio (W/C) was set to be 0.35, and the fine aggregate-to-total aggregate ratio (S/A) was set to be 0.45. Twelve FRLWAC mixtures and a counterpart control fiberless mixture were initially prepared considering the steel fiber types and their V_f. There were three levels of V_f (0.5%, 1.0%, and 1.5%) for each fiber type. Thus, the FRLWAC specimens were denoted using the steel fiber type and V_f level. For example, CSF(C)-1.0 indicates an LWAC mixture reinforced using crimped steel fiber with V_f= 1.0%. Specimen Co refers to the control fiberless mixture.

2.2 Methods

Steel fibers were added after wet mixing of the LWAC. To achieve the targeted minimum slump, a different contents of commercially available polycarboxylate-based superplasticizer was added to each mixture. The slump and air content tests of fresh concrete were conducted according to ASTM C143 and C231, respectively.

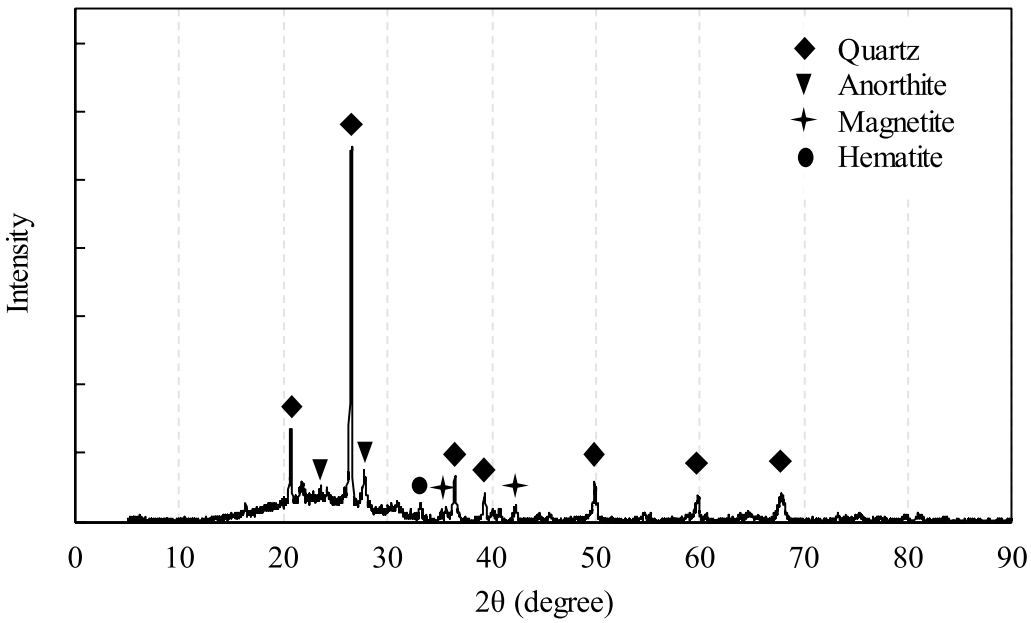

Fig. 1 X-ray diffraction patterns of artificial lightweight aggregates.

Table 1 Physical properties of aggregates.

Aggregate type	Maximum size (mm)	Density (g/cm^3)	Water absorption (%)	Fineness modulus
Lightweight aggregate				
Coarse	20	1.4	14.1	6.41
Fine	5	1.5	10.3	2.90

All specimens were subjected to the vibration casting method specified in ASTM C31. The specimens were cured at a steady temperature and relative humidity of 23 ± 2 °C and 60 ± 5%, respectively, until they were tested at the specified age. The compressive strength, dry densities, splitting tensile strength, and elastic modulus of concrete were measured using 100×200 mm cylindrical specimens, as specified in ASTM C39, C138, C496, and C469, respectively. The relationship between the modulus of rupture and load deflection was measured using prismatic beams having dimensions of $100 \times 100 \times 400$ mm under four-point bending according to ASTM C78 and C1018, respectively.

Fig. 3 shows the fiber pullout test setup used to evaluate the bond stress for each steel fiber type. A load cell with a maximum capacity of 3 kN was used to measure the applied pullout load in the jigs. A dog-bone specimen embedded with one individual fiber was fixed between two jigs, and the pullout test was performed at a speed of 0.02 mm/s (Kim & Yoo, 2020). The pullout of each fiber was commonly induced to occur at the side of the specimen with a 10 mm fiber embedment length. The applied load–slip relationship was evaluated by assuming that the stroke displacement was the slip of the fiber. The average bond stress of the fiber (τ) was calculated by dividing the maximum pullout load by the initial bonding area between the fiber and matrix (Eq. 1):

$$\tau = P_{\max}/\pi d_f L_E, \tag{1}$$

where P_{max} is the maximum pullout load, and L_E is the initial embedded length of the fiber. The mean of the three specimens was applied to all the test results. The compressive strength was measured at 3, 28, and 91 days, and all other tests were performed at 28 days.

3 Results and Discussion

3.1 *Fiber–Matrix Bond Stress*

The increase in the mechanical performance of concrete owing to fiber reinforcement is strongly related to the fiber–matrix interaction and bond strength. Kim and Yoo (2020) reported that the pullout load of the fiber increased significantly when the mechanical anchorage effect was induced owing to the geometric deformation of the steel fiber.

Fig. 4 shows the bond stress–slip relationship for each steel fiber type. Although the L_f of CSF(C) and CSF(S) was 13 mm (Table 2), steel fibers with L_f of 20 mm or more were used in this test to fix the L_E to 10 mm. The bond stress–slip curve was substantially different depending on the type of steel fiber (Fig. 4). Particularly, crimped and hooked-end shapes showed relatively

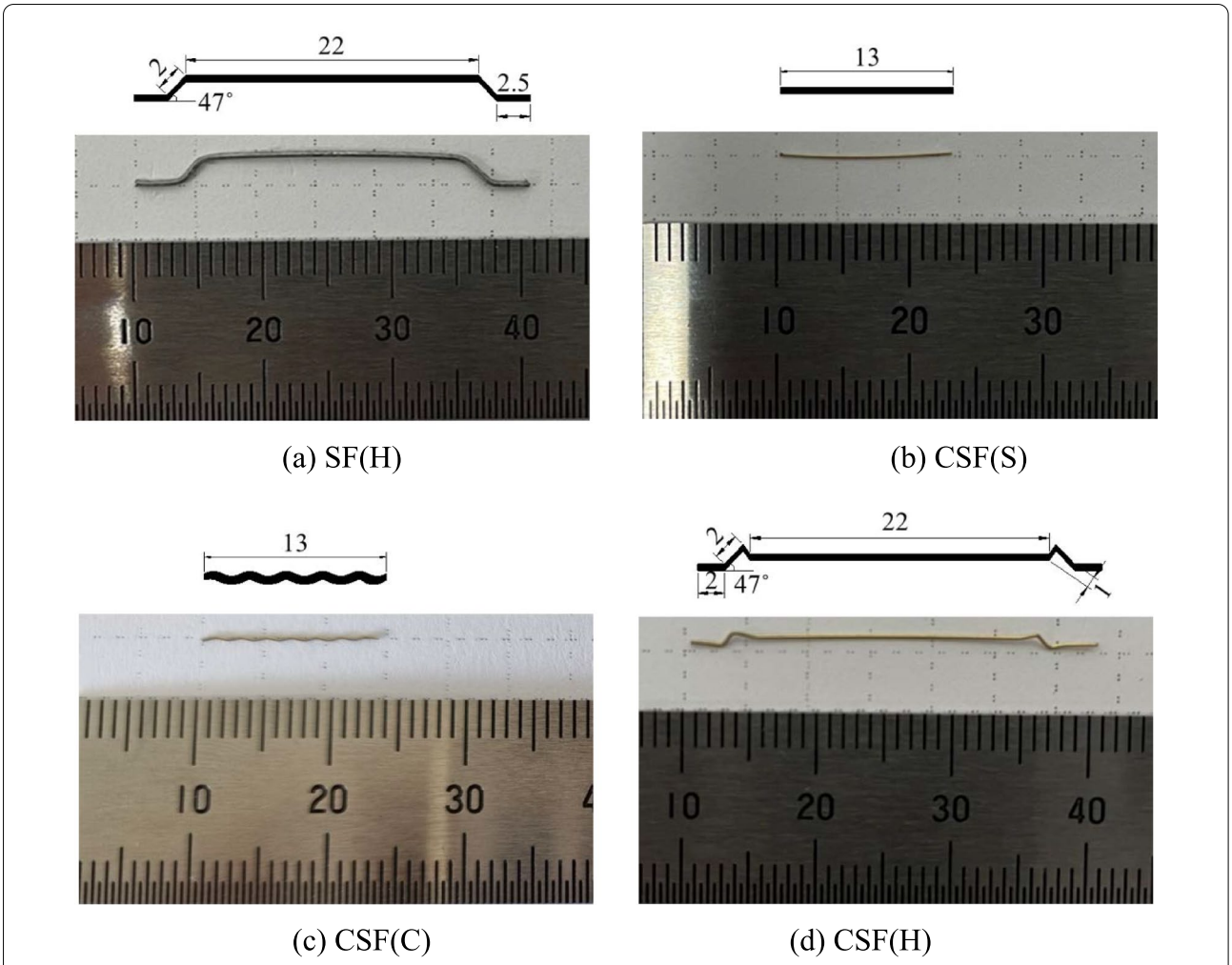

Fig. 2 Typical appearances of steel fibers: **a** SF(H); **b** CSF(S); **c** CSF(C); **d** CSF(H).

Table 2 Properties of steel fibers.

Type	Shape	ρ_f (g/cm^3)	L_f (mm)	d_f (mm)	S_f	F_f (MPa)	τ (MPa)
SF(H)	End-hooked	7.85	35	0.6	58	2240	16.2
CSF(S)	Straight	7.8	13	0.2	65	1220	8.6
CSF(C)	Crimped	7.8	13	0.2	65	1220	11.2
CSF(H)	End-hooked	7.8	30	0.3	100	1220	18.7

ρ_c, L_f, d_f, S_f, F_f, and τ are the density, length, diameter, aspect ratio, tensile strength, and interfacial bond strength between the fiber and cement matrix, respectively.

high τ values owing to their additional mechanical anchorage effects. In contrast, the straight shape was chemically attached to the adjacent cement matrix. This can also be confirmed by the very steep slope of the descending section, i.e., after the peak in the relationship curve of SCF(S). The test results showed that CSF(H) and SF(H) had excellent pullout resistance with maximum τ values of 18.68 and 16.2 MPa, respectively, followed by SCF(C) (11.2 MPa) and SCF(S) (8.6 MPa) (Table 2). Moreover, the results indicated that if other engineering characteristics were excluded and only the influence on the bridging effect between matrices was considered, transforming it into a hooked-end shape can be advantageous. Kim and Yoo (2020) also reported that τ increased in the order of hooked-end, twist, and

Table 3 Mix proportion of concrete.

Specimen	*W/C*	*S/A*	Unit volume weight (kg/m^3)				V_f (%)
			Water	Cement	LWFA	LWCA	
Co	0.35	0.45	180	514	420	479	–
SF(H)-0.5							0.5
SF(H)-1.0							1.0
SF(H)-1.5							1.5
CSF(S)-0.5							0.5
CSF(S)-1.0							1.0
CSF(S)-1.5							1.5
CSF(C)-0.5							0.5
CSF(C)-1.0							1.0
CSF(C)-1.5							1.5
CSF(H)-0.5							0.5
CSF(H)-1.0							1.0
CSF(H)-1.5							1.5

LWFA and LWCA are lightweight fine and coarse aggregates, respectively.

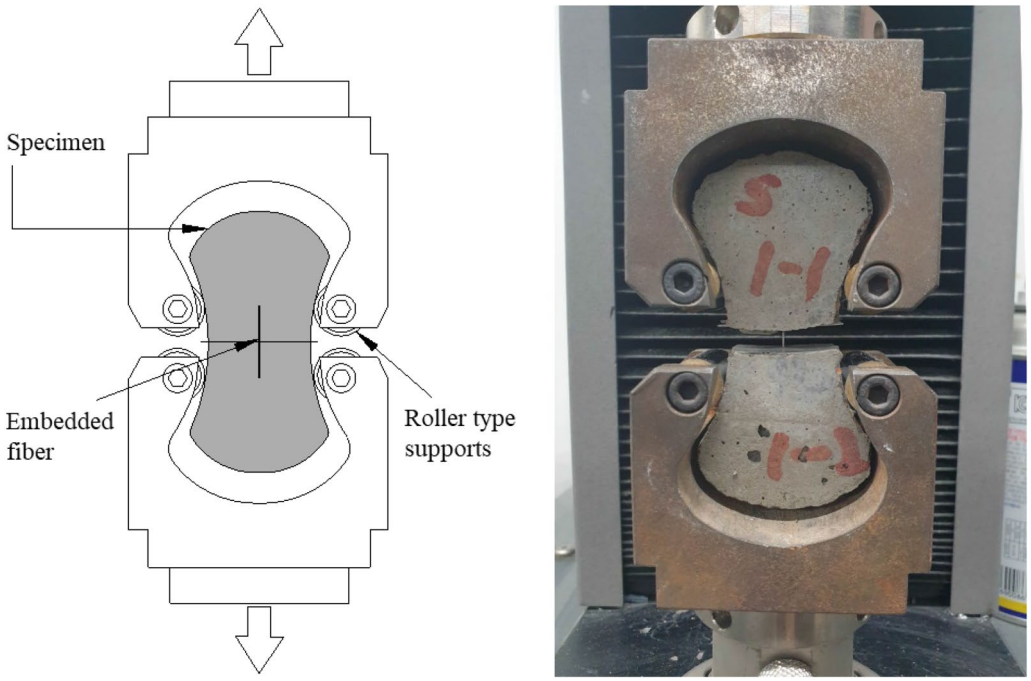

Fig. 3 Fiber pullout test setup.

straight shape, and the averages were 18.6, 17.3, and 10.9, respectively, which was similar to the results seen.

3.2 Workability

In the case of LWAC, a lighter mixture may induce a lower slump (S_l) owing to the effect of gravity between slump tests (Kockal & Ozturan, 2011). Mehta and Monteiro (2017) reported that an SI of approximately 50–75 mm could be sufficient to ensure good workability of LWAC. The test results of the FRLWAC workability showed that the addition of steel fibers tended to lower S_l (Table 4 and Fig. 5). A number of studies, including Bilodeau et. al. (2004); Olivito and Zuccarello (2010), point to the same point of view. Thus, LWAC reinforced with a higher V_f required a higher quantity of superplasticizer to achieve the minimum S_l target value. When V_f

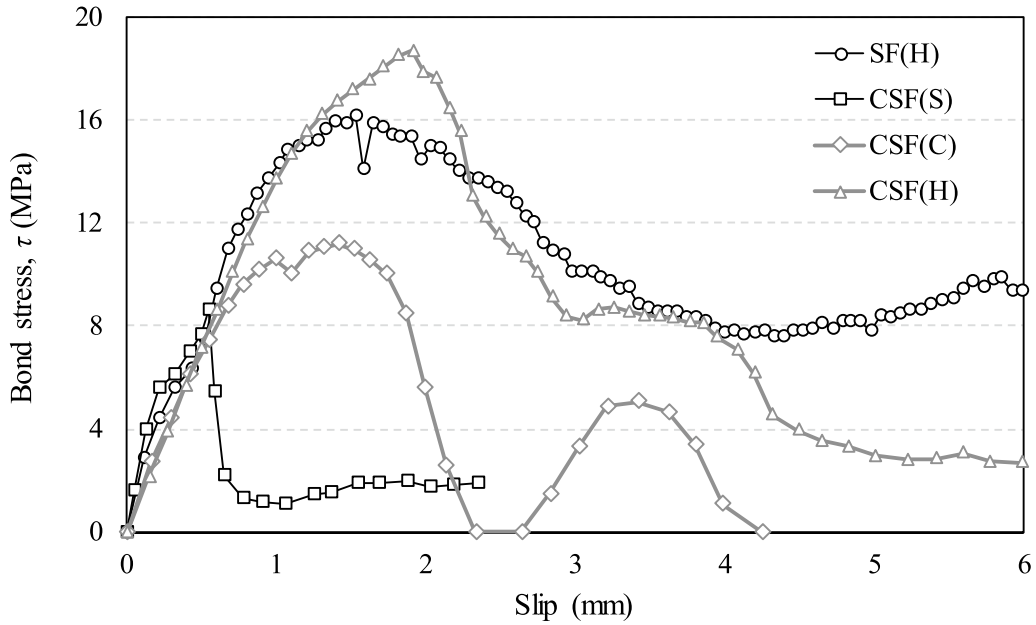

Fig. 4 Bond stress–slip relationship of fibers.

Table 4 Details of test specimens and summary of test results.

Specimens	Details of fibers		R_{sp} (%)	S_l (mm)	A_c (%)	ρ_c (kg/m^3)	$f_c(t)$ (MPa)			f_{sp} (MPa)	f_r (MPa)	E_c (MPa)
	Shape	V_f (%)					3 days	28 days	91 days			
Co	N	0	0.2	165	3.8	1685	30.7	43.4	44.2	3.61	3.14	17,560
SF(H)-0.5	Hooked-end	0.5	0.25	150	3.5	1733	31.9	45.7	47.1	4.12	4.26	17,687
SF(H)-1.0		1.0	0.35	130	3.4	1752	33.4	48.3	51.5	4.54	5.78	18,180
SF(H)-1.5		1.5	0.4	120	3.0	1787	37.4	47.9	54.4	5.20	6.42	18,304
CSF(S)-0.5	Straight	0.5	0.3	140	3.4	1743	34.7	46.4	52.9	4.08	3.95	17,756
CSF(S)-1.0		1.0	0.4	120	3.0	1790	35.7	52.6	55.7	5.41	4.45	19,302
CSF(S)-1.5		1.5	0.45	110	3.2	1803	41.9	55.1	61.8	6.93	5.75	20,145
CSF(C)-0.5	Crimped	0.5	0.45	100	3.4	1740	37.7	46.4	50.5	4.66	4.32	17,757
CSF(C)-1.0		1.0	0.65	70	3.5	1775	41.7	51.8	53.1	5.57	4.87	18,915
CSF(C)-1.5		1.5	0.85	60	3.6	1792	40.1	48.8	49.2	6.56	5.12	18,610
CSF(H)-0.5	Hooked-end	0.5	0.4	130	4.1	1729	34.4	48.1	49.0	4.91	4.85	18,139
CSF(H)-1.0		1.0	0.65	90	3.8	1760	41.5	48.9	54.9	5.92	7.01	18,510
CSF(H)-1.5		1.5	0.75	60	3.7	1790	39.2	49.2	51.2	6.57	7.25	18,940

V_f is the volumetric fraction of fibers, R_{sp} is the ratio of the superplasticizer content relative to the cement mass content, S_l is the slump of fresh concrete, A_c is the air content of fresh concrete, and ρ_c, $f_c(t)$, f_{sp}, f_r, and E_c are the dry density, compressive strength at age t, splitting tensile strength, modulus of rupture, and modulus of elasticity of hardened concrete, respectively.

was increased from 0.5% to 1.5%, the ratio of superplasticizer content (R_{sp}) of SF(H), CSF(C), and SCF(H) mixtures increased by 0.15%, 0.4%, and 0.35%, respectively. However, the measured S_l values tended to decrease. On the other hand, for the CSF(S) mixture, when V_f increased from 0.5% to 1.5%, R_{sp} increased by 1.5%, while S_l decreased by 30 mm. The result indicated that the deformed steel fibers were more unfavorable than the straight-shaped in maintaining the workability of LWAC, because the geometric shape deformation of fibers could accelerate the fiber balling effect owing to the geometry of fibers.

The slump value of fresh concrete can be determined mainly by V_f and R_{sp} (Fig. 5). The regression analysis results showed that the slump value was inversely proportional to V_f and directly proportional to R_{sp}. Therefore,

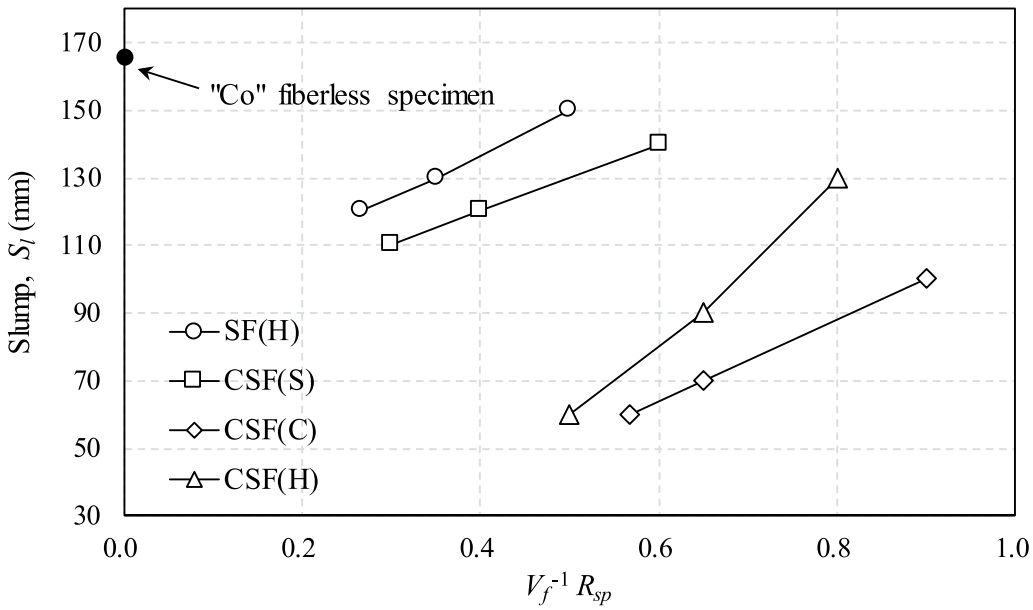

Fig. 5 Regression analysis for slump value of fresh concrete.

it is possible to predict workability using parameters, such as V_f and R_{sp}, in mixtures, where the same fibers are utilized. In securing the workability of FRLWAC, SF(H) and SCF(S) seem to be relatively effective. This might be attributed to the fact that SF(H), with a greater d_f and longer L_f, produces fewer individual fibers, which can degrade the slump of concrete compared to fibers with a smaller diameter.

3.3 Compressive Strength and Oven-Dry Density

Fig. 6 shows the compressive strength and oven-dry density of FRLWAC based on the steel fiber type and V_f. Steel fibers generally increase the compressive strength of LWAC, but the increase is not large. First, the Co mixture showed a compressive strength of 43.4 MPa at an oven-dry density of 1685 kg/m^3 at 28 days. The compressive strength of FRLWAC generally increases as V_f increases. For V_f = 1.5% specimens, the compressive strength of SF(H), CSF(S), CSF(C), and CSF(H) increased by approximately 23.1%, 39.8%, 11.3%, and 15.8%, respectively, compared to the Co mixture. In CSF(S) and SF(H) groups, the addition of fibers had a relatively positive impact on strength improvement, which was closely related to the dispersibility of the fibers. Huang and Zhao (1995) indicated that fiber distribution is very difficult in FRLWAC with a high V_f value. This could result in incomplete compaction and decreased compressive strength. The results of this study showed that CSF(C) and CSF(H), which have a higher quantity of deformed individual fibers, exhibited relatively low strength, i.e., the strength of V_f = 1.5% specimens was lower than that of V_f = 1.0%. The relative oven-dry density (ρ_c) of FRLWAC increased linearly with the V_f value, and this increasing rate was independent of the steel fiber type.

All the ALWC mixtures exhibited a parabolic curve of the compressive strength development. The ratios of 3-day compressive strength relative to 28-day strength ranged between 0.69 and 0.78, 0.68 and 0.76, 0.7 and 0.82, and 0.72 and 0.85 for SF(H), CSF(S), CSF(C), and CSF(H) groups, respectively. The corresponding rages obtained at 91 days are between 1.03 and 1.14, 1.06 and 1.14, 1.01 and 1.08, and 1.02 and 1.12, respectively, for such groups. Hence, the compressive strength development of LWAC was marginally affected by the type, shape, and volume fraction of steel fibers.

3.4 Splitting Tensile Strength

According to ASTM C 330, structural LWACs must have a splitting tensile strength (f_{sp}) of at least 2.0 MPa. The f_{sp} of LWAC was significantly lower than that of NWC with the same compressive strength, because initial cracks can be induced inside the aggregates rather than in the ITZ between the aggregates and matrix (Sim et al., 2013). When V_f was 0.5%, the f_{sp} of CSF(C) and CSF(H) were relatively higher than that of the others (Fig. 7). When V_f increases by 1.0% or more, f_{sp} increases linearly. However, the increase in CSF(S) was relatively higher. Hassanpour et. al. (2012) reported that the f_{sp} of FRLWAC was 16–61% higher than that of fiberless LWAC. $f_{sp}/(f_{sp})_N$, representing the relative f_{sp} value of FRLWAC compared

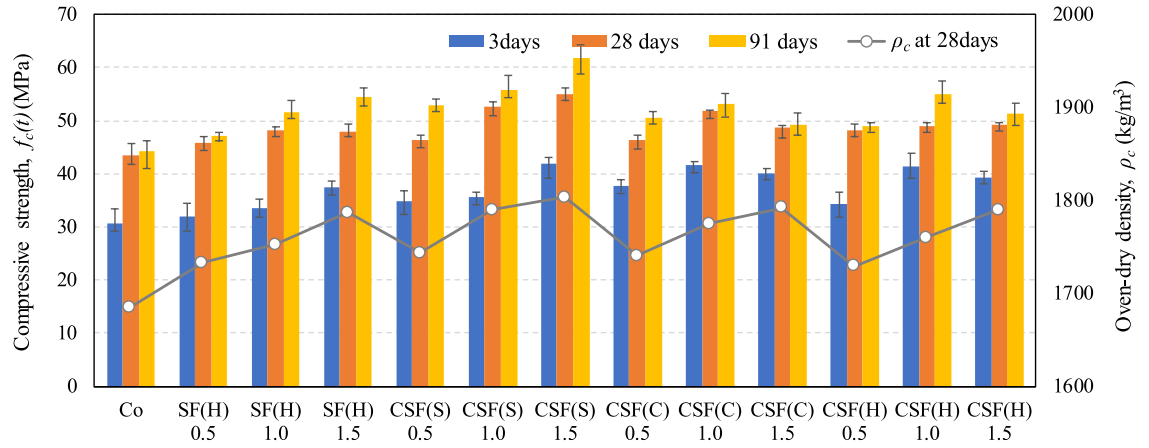

Fig. 6 Compressive strength and oven-dry density of concrete.

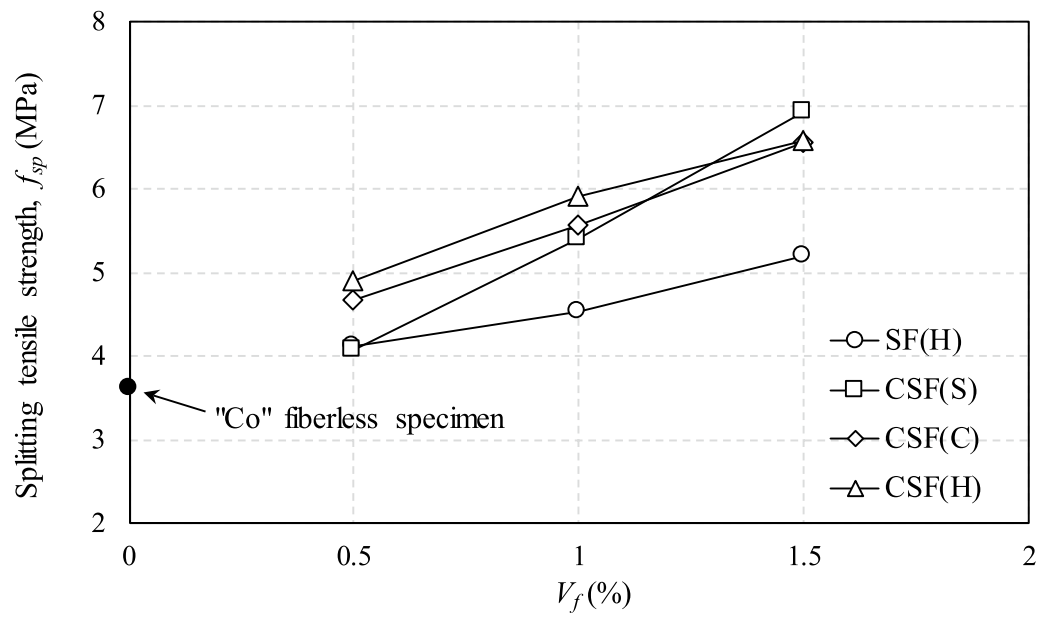

Fig. 7 Splitting tensile strength according to volume fraction of fibers.

to that of the fiberless specimen, was in the range of 1.13–1.92, where the subscript N refers to the fiberless control concrete. The $f_{sp}/(f_{sp})_N$ value ranged from 1.14 to 1.44, 1.13 to 1.92, 1.29 to 1.82, and 1.36 to 1.82 for the SF(H), CSF(S), CSF(C), and CSF(H) groups, respectively (Table 4 and Fig. 8).

Visalvanich and Naaman (1983) defined the characteristics of fibers influencing the performance of FRLWAC as the fiber-reinforced index (β) and expressed it as $\beta = g\tau V_f L_f/d_f$, where g, τ, and L_f/d_f refer to the efficiency factor of discontinuous fibers, interfacial fiber bond strength, and fiber aspect ratio (S_f), respectively. It is difficult to evaluate the factor g independently as g is dependent on several parameters, such as fiber orientation and/or dispersibility, mean embedded length after matrix cracking, and contact area between the fiber and cement matrix. We devised a modified formula for β using S_f, V_f, and τ that measured in Sect. 4.1 for each fiber type.

Fig. 8 shows the results of nonlinear multiple regression (NLMR) of $f_{sp}/(f_{sp})_N$ using modified S_f, V_f, and τ as parameters. The exponent for each variable shown on the X-axis represents the weight of the parameter. The V_f and S_f weights were greater than that of τ for the

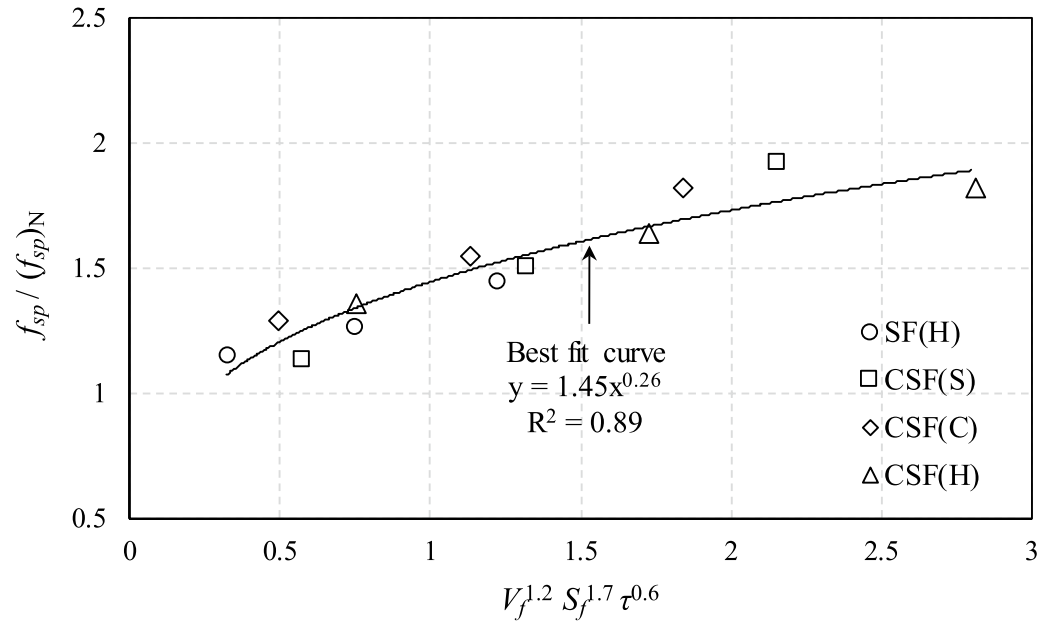

Fig. 8 Regression analysis for normalized splitting tensile strength of concrete.

tensile properties of FRLWAC. The S_f weight was particularly high, because L_f and d_f of steel fibers compared in this study were significantly different. For example, even if V_f was similar, the individual quantity (Q_f) of SCF(S) (d_f=0.2 mm, L_f=13 mm) was 24.2 times higher than that of SF(H) (d_f=0.6 mm, L_f=35 mm), whereas that of SCF(H) (d_f=0.3 mm, L_f=30 mm) was 4.7 times higher. (Note: The Q_f of fibers for V_f=1% (Q_f=10,000,000/π(d_f/2) L_f) were 101,051 for SF(H), 2,448,538 for CSF(S), CSF(C), and 471,570 for CSF(H)). Therefore, it is necessary to treat S_f, which affects the number of individual fibers, as a variable as important as V_f in determining the mechanical properties of FRLWAC. From NLMR analysis using test data sets (Fig. 8), the f_{sp} value for FRLWAC can be optimized as follows:

$$f_{sp} = 1.45\left(V_f^{1.2} \cdot S_f^{1.7} \cdot \tau^{0.6}\right)^{0.26} \cdot (f_{sp})_N. \quad (2)$$

3.5 Flexural Performance

Fig. 9 shows the typical load–deflection behavior of LWAC reinforced with different fiber types at different V_f. There were no data of the control fiberless LWAC after the peak load, because it failed after the initial flexural crack appeared. The descending section of FRLWAC load–deflection curve in Fig. 9 shows the effect of each fiber on the tensile and ductility properties. Many researchers, including Meng and Khayat (2017) and Gesoglu et. al. (2016), have reported that the slope of the descending branch decreases as the bridging capacity or V_f of the fiber increases. The beam with V_f=0.5% showed a similar performance, because the effects of the fibers were small. On the other hand, when V_f was 1.0 or 1.5%, the behavior of the descending section was significantly different depending on the fiber type. The CSF(H)-1.5 beam showed slight hardening or plastic flow performance after initial cracking, but the CSF(S)-1.5 beam showed a very short hardening stage. The CSF(H) group and V_f=1.5% group revealed that the ultimate load (P_n) was higher than the initial cracking load (P_{cr}) by 4.2–18.1%, and the hardening performance was observed after P_{cr}. This results indicated that hooked-end shape fibers were most efficient in enhancing the ductility of FRLWAC.

Fig. 10 shows typical images of the interaction between the cement matrix and steel fibers across a flexural crack, captured for Beams CSF(H)-1.0, SF(H)-1.0, and CSF(S)-1.0. All the beams failed along the primary crack developed at the mid-span, indicating no crack distribution. Most straight shaped fibers were pulled out from the cement matrix, resulting in a wider crack mouth opening displacement (CMOD) in the CSF(S) group, when compared to the other groups using fibers with a longer length. Hooked-end fibers across the crack effectively restricted crack propagation even at the post-peak response because of their good sliding resistance with cement matrix.

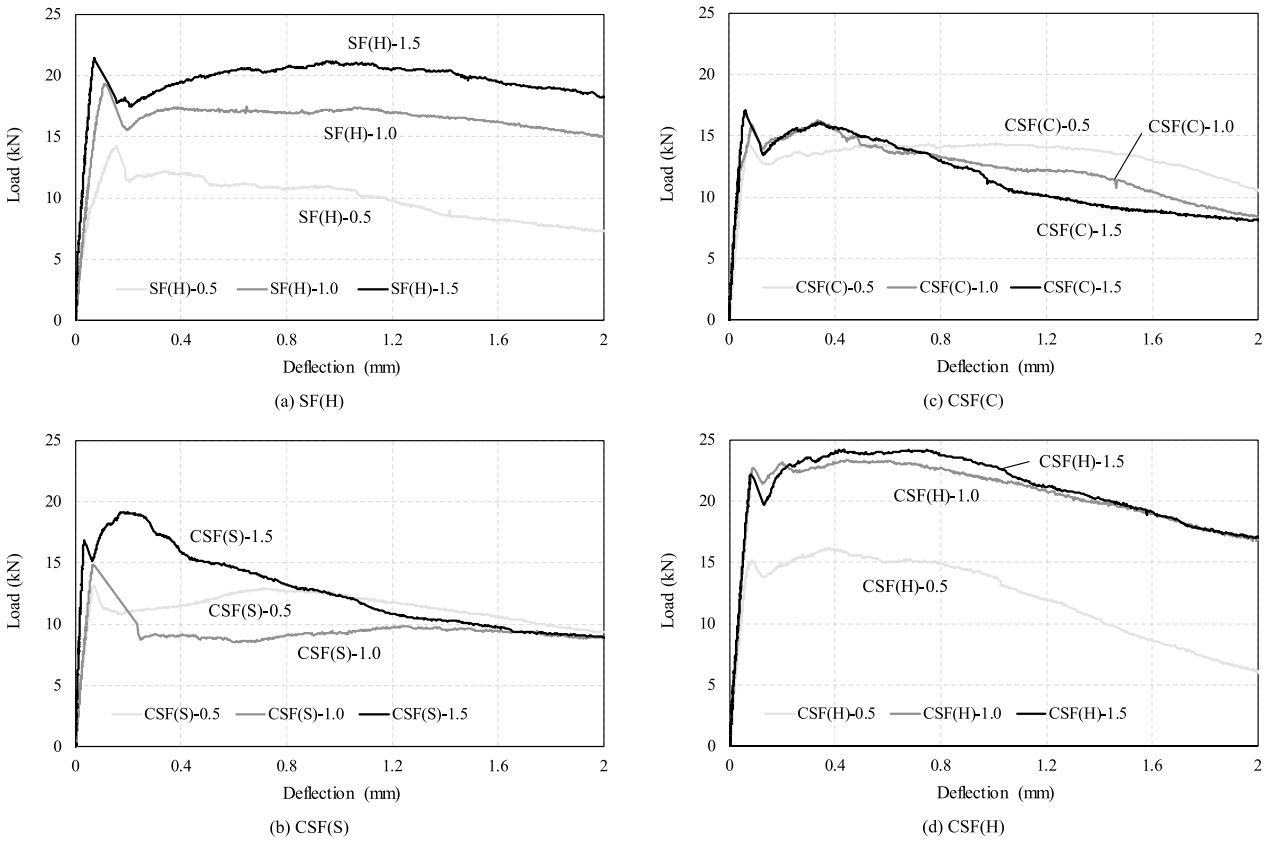

Fig. 9 Typical load–deflection curve of beams under four-point bending test: **a** SF(H); **b** CSF(S); **c** CSF(C); **d** CSF(H).

3.6 Flexural Strength

Fig. 11 and Table 3 show the flexural strength (f_r) of FRLWAC and fiberless control concrete evaluated via the four-point bending test. As expected, regardless of the steel fiber type, f_r values increased with increasing V_f in all FRLWACs. Previous research by (Balendran et. al. (2002); Campione et. al. (2001); Domagala (2011)) have shown that by adding steel fiber to LWAC, the flexural strength of LWAC increased by about 6–38% for $V_f \leq 0.5\%$, 14–182% for $0.5\% < V_f \leq 1\%$ and 42–120% for $1\% < V_f \leq 2\%$. The normalized f_r $(f_r/(f_r)_N)$ values ranged from 1.35 to 2.04, 1.26 to 1.83, 1.38 to 1.63, and 1.54 to 2.31 for the SF(H), CSF(S), CSF(C), and CSF(H) groups, respectively. The f_r values of the SF(H)-1.5 and CSF(H)-1.5 specimens were relatively high, whereas that of the CSF(C)-1.5 specimen showed the lowest value. This trend is somewhat contrasted with the splitting tensile performance of FRLWAC.

When evaluating the flexural performance of FRLWAC, the elastic section before reaching P_{cr} is significantly affected by the strength of the concrete and τ of the reinforcing fibers. However, it is reasonable to assume that most of the τ between the fibers and matrix, which plays a bridging role in the fracture plane, is already lost after initial cracking. The geometric shape of the steel fiber is considered to have a significant influence on determining the ductility capacity and P_n of FRLWAC after reaching P_{cr}. The crack opening displacement of a specimen containing deformed fibers may increase more than that containing a non-deformed fiber owing to the straightening of the deformed shape. The f_r of the CSF(C)-1.5 beam is believed to be relatively low because of this mechanism.

Fig. 12 shows the NLMR analysis results of the flexural strength $(f_r/(f_r)_N)$ of FRLWAC, which was normalized based on the results of the fiberless control concrete. Similar to the previous analysis of $f_{sp}/(f_{sp})_N$, the increasing rate of flexural strength of FRLWAC was predicted using the modified formula for β. The weights of V_f, S_f, and τ, set as parameters of prediction, were 0.6, 0.4, and 0.5, respectively. The f_r values for FRLWAC can be optimized via NLMR analysis as follows:

$$f_r = 1.53\left(V_f^{0.6} \cdot S_f^{0.4} \cdot \tau^{0.5}\right)^{0.53} \cdot (f_r)_N. \quad (3)$$

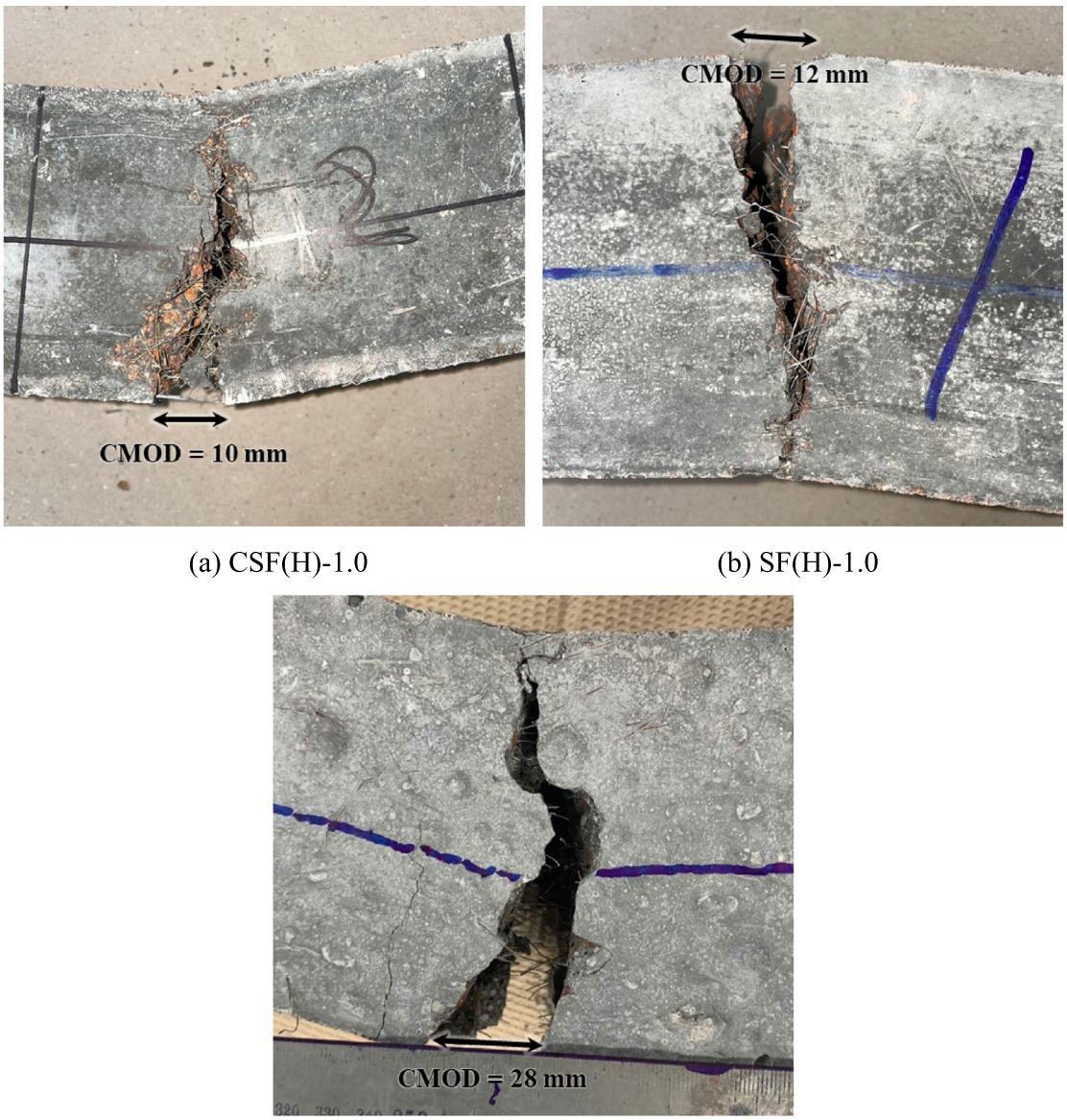

(a) CSF(H)-1.0 (b) SF(H)-1.0

(c) CSF(S)-1.0

Fig. 10 Typical images of crack pattern after four-point bending test: **a** CSF(H)-1.0; **b** SF(H)-1.0; **c** CSF(S)-1.0.

3.7 Modulus of Elasticity

Owing to the low modulus of elasticity (E_c) of the aggregate, E_c of LWAC was 25–50% lower than that of NWC with the same compressive strength. This tendency became more prominent as the LWA content increased. Mehta and Monteiro (2017) suggested that fiber reinforcement in LWAC is not an appropriate solution for improving E_c, especially when V_f is low. Some studies (Campione et. al. (2001); Shafigh et. al. (2011)) reported that E_c could be increased by 6–30% when V_f of FRLWAC was increased.

Fig. 13 shows the NLMR analysis results for the normalized modulus of elasticity ($E_c/\sqrt{f_c(28)}$), where $f_c(28)$ represents the compressive strength measured at the age of 28 days. The experimental values of $E_c/\sqrt{f_c(28)}$ for FRLWAC were between 2607 and 2713. When $E_c/\sqrt{f_c(28)}$ values were predicted for LWAC using the equation given in ACI 318–19, the predicted values ranged between 1959 and 2443; $E_c = \rho_c 0.043\sqrt{f_c(t)}$, where ρ_c is the oven-dry density of the hardened concrete. When comparing the test results of FRLWAC with the predicted values of LWAC, we determined that

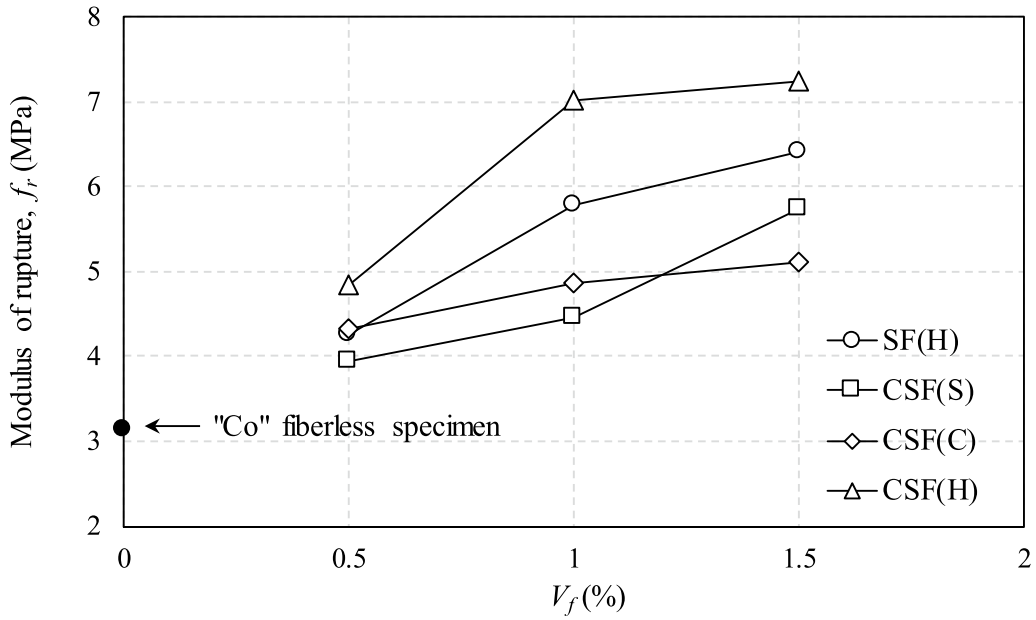

Fig. 11 Modulus of rupture according to the volume fraction of fibers.

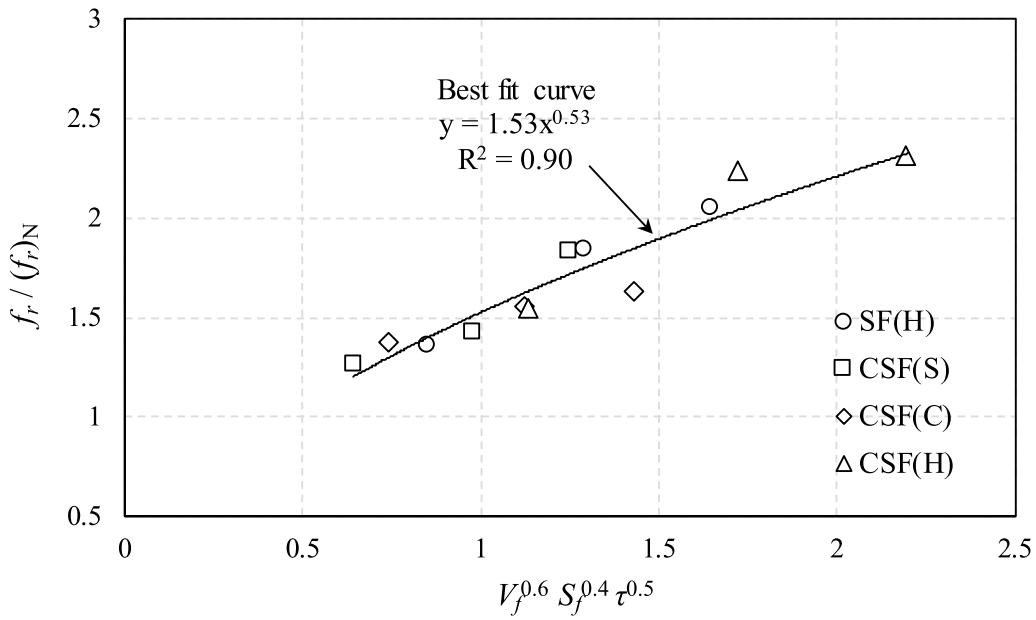

Fig. 12 Regression analysis for normalized modulus of rupture of concrete.

E_c increased by approximately 11–33% because of steel fiber reinforcement, as reported in previous studies. The $E_c/\sqrt{f_c(28)}$ values of the $V_f = 0.5\%$ group were similar regardless of the fiber type (Fig. 13). However, when $V_f = 0.5\%$, $E_c/\sqrt{f_c(28)}$ values of CSF(S)-1.0 and 1.5 were considerably higher than those of the deformed shapes. It is believed that the effect of geometrical deformation of the fiber on the slope of the elastic section of the stress–strain curve is relatively small. However, it can help improve the tensility and ductility of FRLWAC. It is possible to optimize the E_c value of FRLWAC through NLMR analysis (Fig. 13). This is more accurate for FRLWAC with a deformed shape:

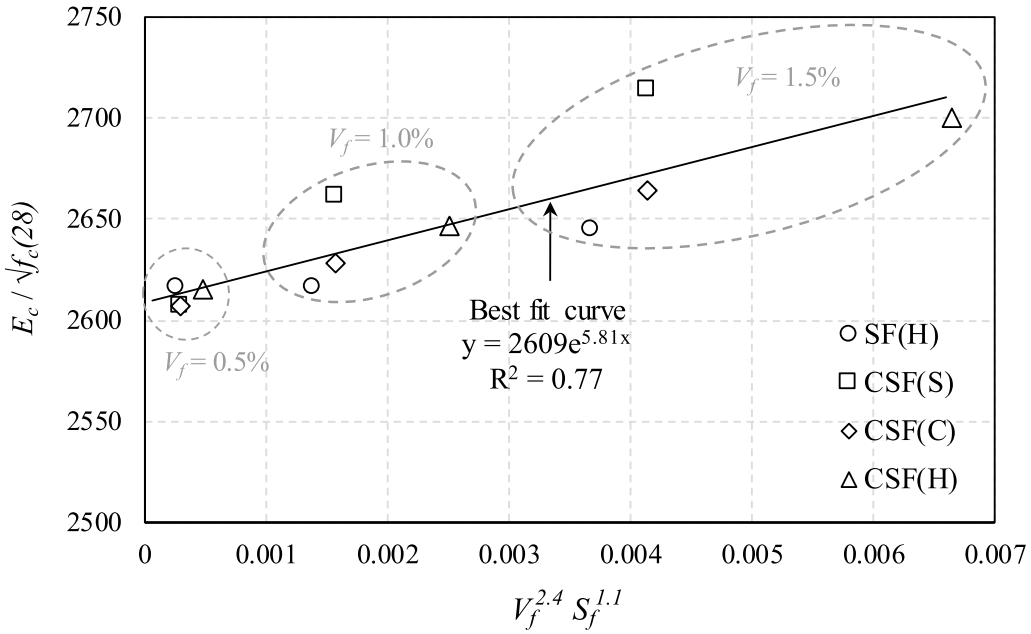

Fig. 13 Regression analysis for normalized elasticity modulus of concrete.

$$E_c = 2609 \exp\left[5.81 \cdot V_f^{2.4} \cdot S_f^{1.1}\right] / f_c(28). \quad (4)$$

4 Conclusions

The present study examined the effects of various steel fibers (conventional macro steel fibers with hooked ends (SF(H)) and copper-coated micro steel fibers (CSF)) on enhancing the mechanical properties of LWAC. The copper-coated micro steel fibers with straight, crimping, and hooked-end shapes were identified as CSF(S), CSF(C), and CSF(H), respectively. While mechanical properties of normal-weight concrete reinforced with the conventional macro steel fibers are commonly available, very few experimental studies have been conducted to examine the various properties of LWAC reinforced with copper-coated micro steel fibers. As a result, no formulations are available to assess the enhanced tensile resistance and toughness of micro steel fiber-reinforced LWAC. Although further test data are required to reliably assess the mechanical properties of micro steel fiber-reinforced LWAC, the following original observations are obtained:

1. Hooked-end steel fibers exhibited greater bond strength and less slip displacement with cement matrix than the straight and crimped steel fibers. In particular, the bond strength of hooked-end micro steel fibers was 15.4% higher than the counterpart macro steel fibers.
2. Straight microsteel fibers were slightly more favorable for preventing the workability degradation of LWAC than the other types of steel fibers at the same volume fraction.
3. The compressive strength development of LWAC was marginally affected by the type, shape, and volume fraction of fibers.
4. The deformed steel fibers were more effective than the straight fibers in enhancing the splitting tensile and flexural strengths of LWAC. Particularly, LWAC reinforced with CSF(H) exhibited higher flexural strength and flexural hardening response than the counterpart LWAC specimens with SF(H) or CSF(C).
5. The effect of various steel fibers on the enhancement of the splitting tensile and flexural strengths of LWAC could be formulated as a function of V_f, S_f, and τ, as expressed in the following: $f_{sp} = 1.45\left(V_f^{1.2} \cdot S_f^{1.7} \cdot \tau^{0.6}\right)^{0.26} (f_{sp})_N$; $f_r = 1.53\left(V_f^{0.6} \cdot S_f^{0.4} \cdot \tau^{0.5}\right)^{0.53} (f_r)_N$, where $(f_{sp})_N$ and $(f_r)_N$ are the splitting tensile and flexural strengths of fiber-less LWAC.

Acknowledgements

This work was supported by the Korea Agency for Infrastructure Technology Advancement (KAIA) grant funded by the Ministry of Land, Infrastructure and Transport (Grant 22NANO-C156177-03)

Author contributions
The first author, KHY, planned and supervised the project, and reviewed this manuscript. The corresponding author, HYK, analyzed the data and wrote this manuscript. HJL performed the experiments and provided the experimental data. All authors read and approved the final manuscript.

Author's information
K. H. Yang is a professor at Kyonggi University, South Korea. He received the Scientific Technician Medal for Most Meritorious Achievement in 2010 from the National Research Foundation of Korea. His recent research interests include the development of sustainable concrete materials and structural technology.
H. Y. Kim is a research professor at Kyonggi University, South Korea. He received his BE, MS, and PhD in the Department of Architecture Engineering at Dankook University. His research work includes the development of design models of sustainable concrete using various recycling materials.
H. J. Lee is a graduate student at Kyonggi University, South Korea. Her interest focuses on examining the mechanical properties of lightweight aggregate concrete.

Availability of data and materials
All data generated or analyzed during this study are included in this published article.

Decalarations

Competing interests
The authors declare that they have no competing interests.

Received: 3 February 2022 Accepted: 2 June 2022
Published online: 13 September 2022

References

ACI Committee 213. (2014). *Guide for Structural Lightweight Aggregate Concrete (ACI 213R-14). American Concrete Institute*. American Concrete Institute. https://doi.org/10.14359/7576
ASTM C150/C150M. (2011). *Standard specification for portland cement*. ASTM International: ASTM International. https://doi.org/10.1002/jbm.b.31853
ASTM C330, C330M. (2017). Standard specification for lightweight aggregates for structural concrete. ASTM International. *ASTM International*. https://doi.org/10.1520/C0330
Balendran, R. V., Zhou, F. P., Nadeem, A., & Leung, A. Y. T. (2002). Influence of steel fibres on strength and ductility of normal and lightweight high strength concrete. *Building and Environment, 37*(12), 1361–1367.
Bilodeau, A., Kodur, V. K. R., & Hoff, G. C. (2004). Optimization of the type and amount of polypropylene fibres for preventing the spalling of lightweight concrete subjected to hydrocarbon fire. *Cement and Concrete Composites, 26*(2), 163–174. https://doi.org/10.1016/S0958-9465(03)00085-4
Campione, G., Miraglia, N., & Papia, M. (2001). Mechanical properties of steel fibre reinforced lightweight concrete with pumice stone or expanded clay aggregates. *Materials and Structures, 34*(4), 201–210. https://doi.org/10.1007/BF02480589
Domagala, L. (2011). Modification of properties of structural lightweight concrete with steel fibres. *Journal of Civil Engineering and Management, 17*(1), 36–44. https://doi.org/10.3846/13923730.2011.553923
Dupont, D., & Vandewalle, L. (2005). Distribution of steel fibres in rectangular sections. *Cement and Concrete Composites, 27*(3), 391–398. https://doi.org/10.1016/j.cemconcomp.2004.03.005
Gesoglu, M., Güneyisi, E., Muhyaddin, G. F., & Asaad, D. S. (2016). Strain hardening ultra-high performance fiber reinforced cementitious composites: effect of fiber type and concentration. *Composites Part b: Engineering, 103*, 74–83. https://doi.org/10.1016/j.compositesb.2016.08.004
Hamoush, S., Abu-Lebdeh, T., & Cummins, T. (2010). Deflection behavior of concrete beams reinforced with PVA micro-fibers. *Construction and Building Materials, 24*(11), 2285–2293.
Hassanpour, M., Shafigh, P., & Mahmud, H. B. (2012). Lightweight aggregate concrete fiber reinforcement–a review. *Construction and Building Materials, 37*, 452–461. https://doi.org/10.1016/j.conbuildmat.2012.07.071
Huang, C., & Zhao, G. (1995). Properties of steel fibre reinforced concrete containing larger coarse aggregate. *Cement and Concrete Composites, 17*(3), 199–206. https://doi.org/10.1016/0958-9465(95)00012-2
Kang, S. T., Lee, Y., Park, Y. D., & Kim, J. K. (2010). Tensile fracture properties of an Ultra High Performance Fiber Reinforced Concrete (UHPFRC) with steel fiber. *Composite Structures, 92*(1), 61–71. https://doi.org/10.1016/j.compstruct.2009.06.012
Kim, D. J., Park, S. H., Ryu, G. S., & Koh, K. T. (2011). Comparative flexural behavior of Hybrid Ultra High Performance Fiber Reinforced Concrete with different macro fibers. *Construction and Building Materials, 25*(11), 4144–4155. https://doi.org/10.1016/j.conbuildmat.2011.04.051
Kim, M. J., & Yoo, D. Y. (2020). Analysis on enhanced pullout resistance of steel fibers in ultra-high performance concrete under cryogenic condition. *Construction and Building Materials, 251*, 118953. https://doi.org/10.1016/j.conbuildmat.2020.118953
Kockal, N. U., & Ozturan, T. (2011). Strength and elastic properties of structural lightweight concretes. *Materials and Design, 32*(4), 2396–2403. https://doi.org/10.1016/j.matdes.2010.12.053
Lee, K. H., Yang, K. H., Mun, J. H., & Kwon, S. J. (2019). Mechanical properties of concrete made from different expanded lightweight aggregates. *ACI Materials Journal, 116*(2), 9–19. https://doi.org/10.14359/51712265
Li, J. J., Wan, C. J., Niu, J. G., Wu, L. F., & Wu, Y. C. (2017). Investigation on flexural toughness evaluation method of steel fiber reinforced lightweight aggregate concrete. *Construction and Building Materials, 131*, 449–458. https://doi.org/10.1016/j.conbuildmat.2016.11.101
Li, J., Zhao, E., Niu, J., & Wan, C. (2021). Study on mixture design method and mechanical properties of steel fiber reinforced self-compacting lightweight aggregate concrete. *Construction and Building Materials, 267*, 121019. https://doi.org/10.1016/j.conbuildmat.2020.121019
Mays, G. C., & Barnes, R. (1991). Performance of lightweight aggregate concrete structures in service. *Structural Engineer, 69*, 351–361.
Mehta, P. K., & Monteiro, P. J. M. (2017). *Concrete microstructure, properties and materials*.
Meng, W., & Khayat, K. H. (2017). Improving flexural performance of ultra-high-performance concrete by rheology control of suspending mortar. *Composites Part b: Engineering, 117*, 26–34. https://doi.org/10.1016/j.compositesb.2017.02.019
Okeh, C. A. O., Begg, D. W., Barnett, S. J., & Nanos, N. (2019). Behaviour of hybrid steel fibre reinforced self compacting concrete using innovative hooked-end steel fibres under tensile stress. *Construction and Building Materials, 202*, 753–761.
Olivito, R. S., & Zuccarello, F. A. (2010). An experimental study on the tensile strength of steel fiber reinforced concrete. *Composites Part b: Engineering, 41*(3), 246–255. https://doi.org/10.1016/j.compositesb.2009.12.003
Park, S. H., Kim, D. J., Ryu, G. S., & Koh, K. T. (2012). Tensile behavior of ultra high performance hybrid fiber reinforced concrete. *Cement and Concrete Composites, 34*(2), 172–184. https://doi.org/10.1016/j.cemconcomp.2011.09.009
Shafigh, P., Mahmud, H., & Jumaat, M. Z. (2011). Effect of steel fiber on the mechanical properties of oil palm shell lightweight concrete. *Materials and Design, 32*(7), 3926–3932. https://doi.org/10.1016/j.matdes.2011.02.055
Sim, J. I., Yang, K. H., Kim, H. Y., & Choi, B. J. (2013). Size and shape effects on compressive strength of lightweight concrete. *Construction and Building Materials, 38*, 854–864. https://doi.org/10.1016/j.conbuildmat.2012.09.073
Turk, K., Bassurucu, M., & Bitkin, R. E. (2021). Workability, strength and flexural toughness properties of hybrid steel fiber reinforced SCC with high-volume fiber. *Construction and Building Materials, 266*, 120944.
Visalvanich, K., & Naaman, A. E. (1983). Fracture model for fiber reinforced concrete. *Journal of the American Concrete Institute, 80*(2), 128–138. https://doi.org/10.14359/10712
Wu, Z., Khayat, K. H., & Shi, C. (2018). How do fiber shape and matrix composition affect fiber pullout behavior and flexural properties of UHPC. *Cement and Concrete Composites, 90*(2017), 193–201. https://doi.org/10.1016/j.cemconcomp.2018.03.021

Publisher's Note